Oxidation of butane over vanadium–phosphorus oxides of P/V $\geqslant 2$

Daxiang Wang [*], Mayfair C. Kung and Harold H. Kung [**]

Department of Chemical Engineering, Northwestern University, 2145 Sheridan Road, Evanston, IL 60208-3120, USA
E-mail: hkung@nwu.edu

Received 9 September 1999; accepted 10 January 2000

Two mixed oxides of vanadium and phosphorus, with phosphorus to vanadium atomic ratio (P/V) about 2 and 2.4, were studied as catalysts for selective oxidation of butane to maleic anhydride. The sample with P/V about 2 was poorly crystalline, contained a small amount of V(V), and oxidized butane to maleic anhydride with about 50% selectivity. The sample with P/V about 2.4 contained well crystalline $VO(PO_3)_2$ phase, but it deactivated with time-on-stream with the formation of $V(PO_3)_3$. The results suggested that the two samples differed greatly in their rates of oxidation of the vanadium ions.

Keywords: butane oxidation, maleic anhydride, vanadyl metaphosphate, VPO catalysts

1. Introduction

Vanadium–phosphorus oxide (VPO) is the commercial catalyst for the selective oxidation of butane to maleic anhydride (MA) [1]. Even though the bulk phase of this catalyst is composed of well-crystallized vanadyl pyrophosphate ($(VO)_2P_2O_7$), the best industrial catalysts always have phosphorus to vanadium atomic ratios (P/V) slightly higher than unity [1,2]. The status of the extra phosphorus and its effect on the catalytic performance has long been one of the most interesting topics in this catalytic system. Surface enrichment of phosphorus was observed by X-ray photoelectron spectroscopy and other techniques [3–5], and recent results have suggested strongly that the crystalline $(VO)_2P_2O_7$ phase is not necessary for high selectivity and activity [6,7]. For example, Hutchings et al. [3] observed that, on the surface of a well-crystallized vanadyl pyrophosphate with bulk P/V ratios between 1 and 1.2, surface enrichment of phosphorus results in surface P/V ratios near 2. Therefore, studies of VPO catalysts with bulk P/V ratios higher than unity have been of interest among researchers [8–12].

A general dependence of the catalytic performance on the P/V ratio near unity is that increasing P/V ratio improves the selectivity to MA while decreasing activity. In our previous studies over silica-supported VPO catalysts, it was observed that the selectivity for maleic anhydride in butane oxidation increased from about 25% for catalysts with a P/V ratio of unity to about 50% for a P/V ratio of about two [8,9].

However, controversial results have been reported on the performance of VPO catalysts with P/V ratios near or above two, especially for the catalysts derived from vanadyl dihydrogen phosphate, $VO(H_2PO_4)_2$. Morishige et al. obtained a low activity with 64.5% selectivity for butane to maleic anhydride [10]. Sananes et al. reported 100% selectivity toward partial oxidation products (mainly maleic anhydride) at very low conversions [11,12], whereas Guliants et al. found the compound to be completely inactive for butane oxidation reaction [13]. Even with these controversies in the literature, continual efforts are still being made to improve $VO(H_2PO_4)_2$ as selective oxidation catalysts [14,15].

In this paper, two catalysts prepared from precursors of different P/V ratios but containing crystalline $VO(H_2PO_4)_2$ were characterized. The implications of their different catalytic properties on the nature of the active phase are discussed.

2. Experimental

2.1. Catalyst preparation

$VO(H_2PO_4)_2$ was prepared by an aqueous procedure based on the method of Sananes et al. [11]. Aqueous H_3PO_4 was mixed with V_2O_4 and allowed to sit overnight. The deep blue, glassy mixture was then refluxed between 180 and 200 °C for 1–6 h until the suspension became predominately pale blue. The suspension was centrifuged. After decanting the liquid, the solid was redispersed with diethyl ether. The centrifugation and resuspension with a new batch of ether was repeated for five times to remove H_3PO_4. Finally, the pale blue solid was dried at 100 °C overnight. The resulting precursor is referred to as precursor A. It had a P/V ratio of 2.05 ± 0.08, as analyzed by inductively coupled plasma (ICP).

Precursor B was prepared by three times re-crystallization of the pale blue mixture after reflux by dissolving the solid in water. After the final recrystallization, the solid was washed with diethyl ether. Precursor B was bluish gray after drying at 100 °C overnight. The P/V ratio of precursor B was 2.40 ± 0.08.

---

[*] Present address: Center for Catalytic Science and Technology, University of Delaware, Newark, DE 19716, USA. E-mail: wangd@che.udel.edu

[**] To whom correspondence should be addressed.

After activation under reaction conditions for 2 h, the BET surface area of the P/V = 2.05 sample was 5 m^2/g, and of the P/V = 3.4 sample it was 3.6 m^2/g.

2.2. Catalytic test

Catalytic tests were carried out using a fixed-bed microreactor. Gas mixtures of $C_4H_{10}/O_2/He$ of 2/24/74 or 1.0/10.2/88.8 (vol%) were used at flowrates of 70 ml/min and 20 ml/min, respectively. About 0.8 or 1.7 g catalyst with particle size between 20 and 40 mesh was used. When the catalyst was activated *in situ*, the temperature was increased from room temperature to 100 °C at 2 °C/min, then held at 100 °C for 1 h. The temperature was then increased to the reaction temperature at 10 °C/min. In some experiments, precursor A was activated by calcination in air at 500 °C for 24 h. The effluent gases were analyzed in the same way as described in the literature [8,9].

2.3. Characterization

The precursors and catalysts were characterized by X-ray diffraction (XRD) on a Rigaku powder diffractometer using Cu Kα radiation and Ni filter. LiF was used as an internal standard to calibrate the peak positions. The spectra were collected under ambient conditions, including those for catalysts after reaction. Laser Raman spectra (LRS) were collected using Ar ion laser excitation (514.5 nm). The power of the laser at the sample was 25 mW. The spectra were collected under ambient conditions. The phosphorus to vanadium ratios were determined by inductively coupled plasma (ICP) after dissolving the solid sample in water. The diffuse reflectance spectra (DRS) were collected under ambient conditions using polytetrafluoroethylene as the reference.

3. Results and discussion

3.1. $VO(H_2PO_4)_2$ precursors

Figure 1 shows the XRD patterns of precursors A and B. Both precursors showed only sharp diffraction peaks for $VO(H_2PO_4)_2$ [11]. The relative intensities of the peaks were roughly the same for both samples. The Raman spectrum of precursor A (shown in figure 2) showed a main peak at 937 cm^{-1}, which is in agreement with the literature data for $VO(H_2PO_4)_2$ [11,12]. Figure 3 shows the diffusive reflectance spectrum of precursor A. There were three broad absorption bands at 205, 378 and 618 nm. According to Villeneuve et al. [16], they can be attributed to the $e_\pi \rightarrow e_\pi^*$, $^2B_2 \rightarrow {}^2A_1$, and $^2B_2 \rightarrow {}^2B_1$ transitions of the V(IV) ion in $VO(H_2PO_4)_2$, respectively. There was also a shoulder at about 275 nm. A similar spectrum was obtained for precursor B.

The ICP analyses indicated that precursors A and B had P/V atomic ratios of 2.05 ± 0.08 and 2.40 ± 0.08, respectively. Within experimental error, precursor A had the stoichiometric P/V ratio of $VO(H_2PO_4)_2$. The higher P/V ratio for precursor B suggested the presence of extra phosphoric acid in this precursor, that was probably intercalated

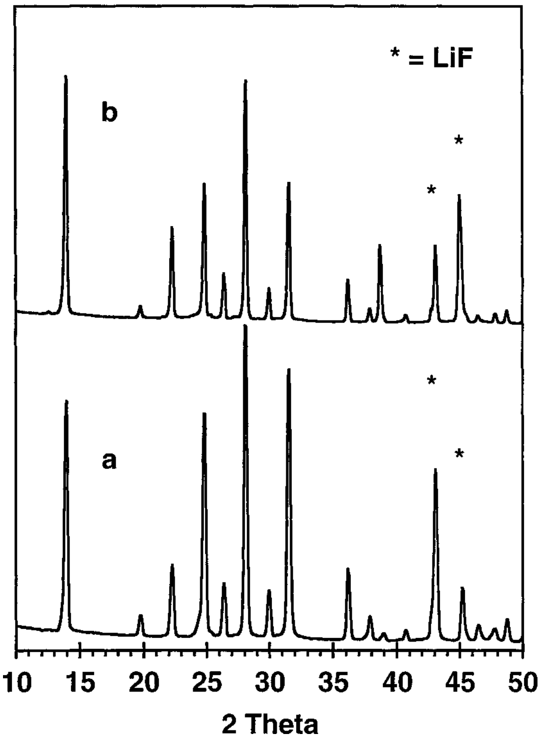

Figure 1. XRD patterns of $VO(H_2PO_4)_2$ precursors: (a) precursor A and (b) precursor B.

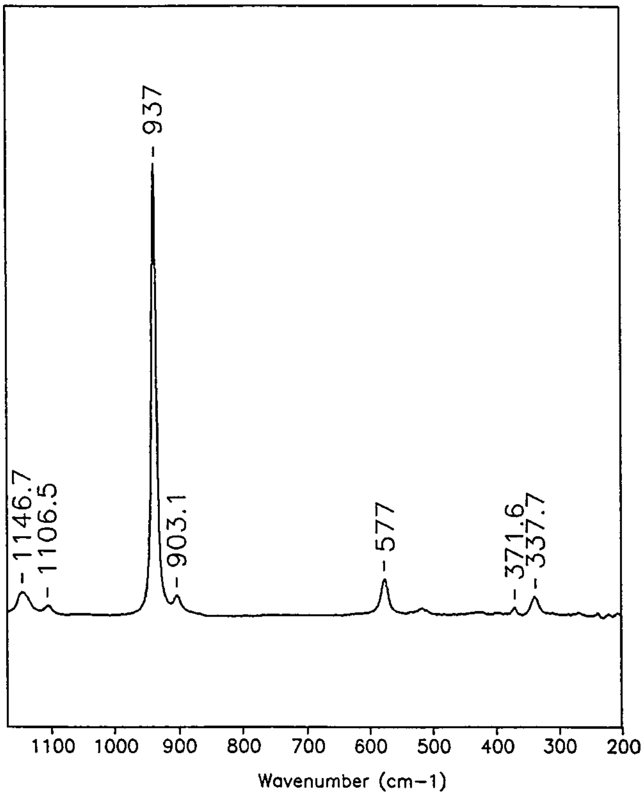

Figure 2. LRS of $VO(H_2PO_4)_2$, precursor A.

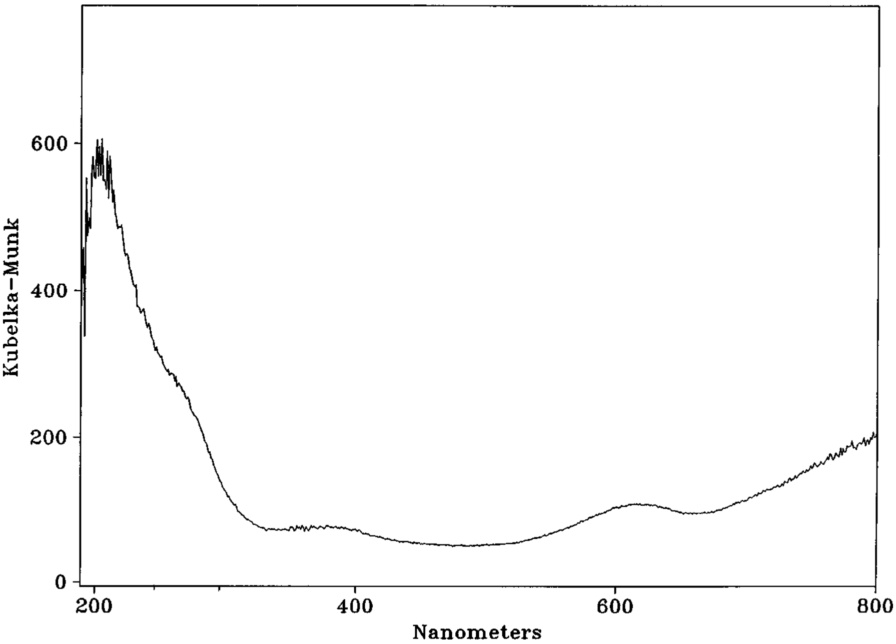

Figure 3. DRS of $VO(H_2PO_4)_2$, precursor A.

in the crystalline structure of $VO(H_2PO_4)_2$ as suggested by Lodwig [17]. Results of activation experiments (shown later) indicated that the occluded phosphoric acid affected the transformation of $VO(H_2PO_4)_2$ to crystalline $VO(PO_3)_2$.

3.2. Catalysts derived from precursor A

3.2.1. Catalyst structure

In order to obtain a well-crystallized $VO(PO_3)_2$, activation of the precursor was attempted using various procedures, such as calcination in dry air, moisture air, or nitrogen, or under reaction conditions. No pure crystal phase was obtained in any of these treatments. Figure 4 shows the XRD patterns of samples after activation by calcination in air at 500 °C or under reaction conditions. A common feature in these patterns is the presence of a very broad peak spanning $2\theta = 15$–$35°$, indicating the presence of an amorphous phase.

The pattern for the air-calcined catalyst also showed peaks at $2\theta = 22.4°$, $22.9°$, and $24.2°$ in addition to other small peaks (figure 4(a)). They could be all assigned to $VO(PO_3)_2$ [13,18,19]. Thus, this catalyst contained a mixture of an amorphous phase and crystalline $VO(PO_3)_2$. A comparison of curves (a) and (b) in figure 4 showed that there were no obvious changes in the XRD pattern of the catalyst after reaction. However, the catalyst did change its color from yellowish brown to brown after reaction. This change could be reversed by calcining the used catalyst in air at 500 °C for 24 h without changing its XRD pattern. From our experience, the color change corresponded to the reduction of vanadium ions from V(V) to V(IV) and/or V(III) [20].

For the catalyst activated *in situ*, there were three small peaks at $2\theta = 14.3°$, $23.9°$, and $28.8°$ (see figure 4(c)). They should be assigned to $VOPO_4{\cdot}2H_2O$ ($2\theta = 28.8°$, 24° and the hydrate peak at $2\theta < 15°$) [15,21]. In addition, there was a relatively large broad peak centered at about $2\theta = 22°$, which indicated that this sample contained a larger portion of amorphous material than the air-calcined sample.

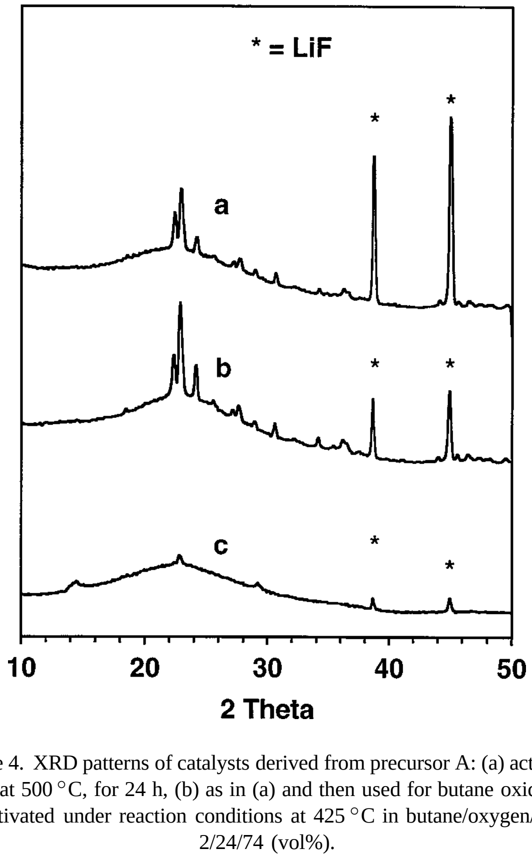

Figure 4. XRD patterns of catalysts derived from precursor A: (a) activated in air at 500 °C, for 24 h, (b) as in (a) and then used for butane oxidation, (c) activated under reaction conditions at 425 °C in butane/oxygen/He = 2/24/74 (vol%).

The LRS spectra of the samples obtained by calcination in air or activated in a reaction mixture are shown

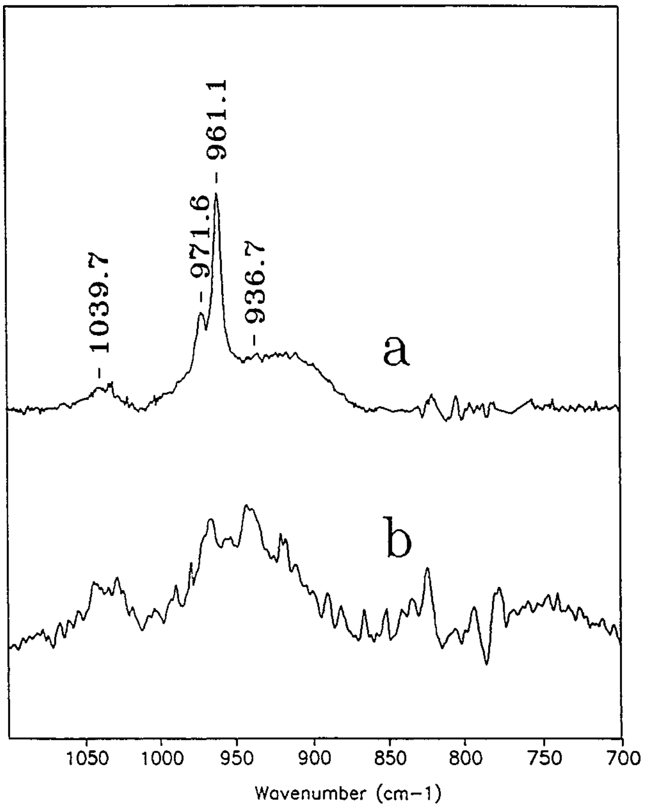

Figure 5. LRS spectra of VPO catalysts derived from precursors A: (a) activated in air at 500 °C, for 24 h, (b) activated under reaction conditions at 425 °C in butane/oxygen/He = 2/24/74 (vol%).

in figure 5. In the spectrum for catalyst activated in air (figure 5(a)), there were four absorption peaks. The peak at 1038 cm^{-1} indicated the presence of an α-$VOPO_4$-like compound [22]. The sharp peaks at 971.6 and 961.1 cm^{-1} can be attributed solely to the crystalline phase of $VO(PO_3)_2$. The slight difference in peak positions observed here with the literature data could be due to interference from the broad background peak. The broad peak at about 936 cm^{-1} could be formed by the overlap of peaks at 957 cm^{-1} (for $VO(PO_3)_2$) and 926 cm^{-1} (for the α-$VOPO_4$-like compound).

The spectrum for the catalyst activated under reaction conditions was much less well resolved (figure 5(b)). This is in agreement with the XRD results that there was a minor amount of crystalline materials in the sample. In general, this spectrum was in agreement with the presence of α-$VOPO_4$-like compound and $VO(PO_3)_2$.

These characterization results showed that crystalline $VO(PO_3)_2$ was formed more readily by air calcination than under reaction conditions. A substantial fraction of the sample was amorphous to X-ray diffraction. The color change of the air-calcined sample after reaction was indicative of some reduction of V(V) to V(IV) or V(III), which was present in the amorphous phase. Activation under reaction conditions also resulted in some oxidation of V(IV) in the precursor to V(V). The resulting sample was less crystalline than the air-calcined sample.

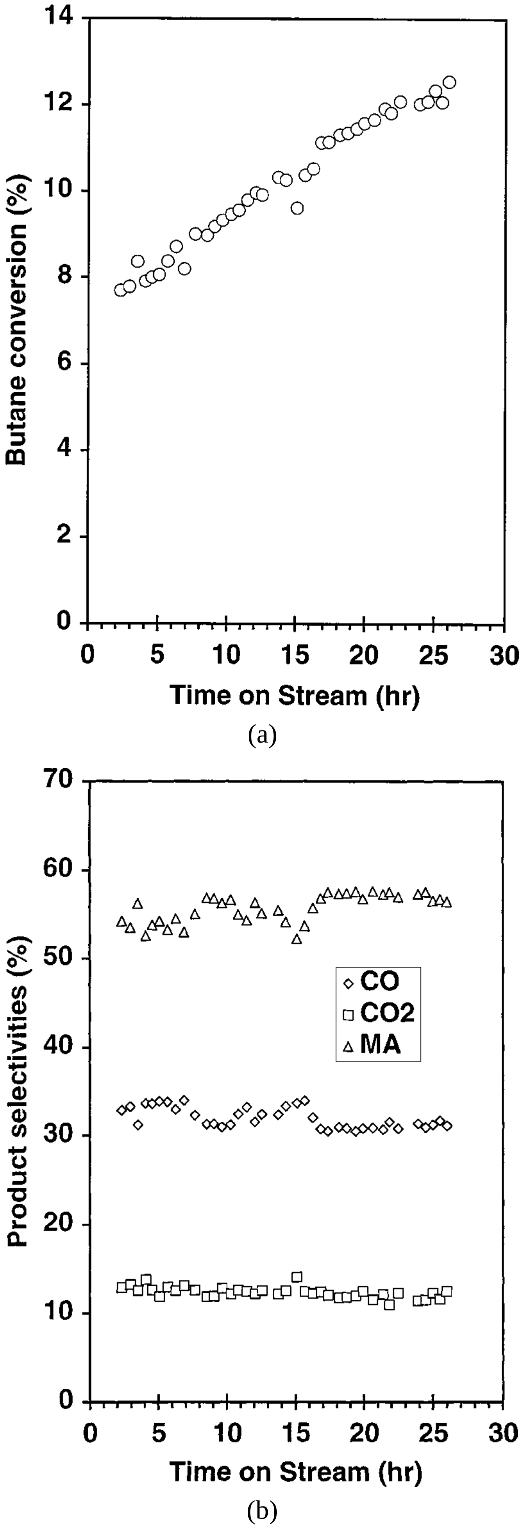

Figure 6. Butane oxidation on precursor A activated *in situ*. Reaction conditions: 485 °C, catalyst weight 0.8 g, total gas flow rate 70 ml/min, gas composition: butane/oxygen/He = 2/24/74 (vol%). (a) Butane conversion and (b) product selectivities.

3.2.2. Catalytic activity

The activity with time on stream of the catalysts from precursor A depended on the activation procedures. Figure 6 (a) and (b) shows the reaction results for a catalyst from precursor A activated *in situ*. The first data point was recorded after the catalyst had been activated at 485 °C for about 2 h in a gas mixture of $C_4H_{10}/O_2/He = 2/24/74$ (vol%) at total flowrate of 70 ml/min. Butane conversion increased continuously with time-on-stream, from 8 to 12% after 24 h. The selectivity to maleic anhydride was stable at about 55% during the entire period.

On the other hand, the behavior of precursor A after activation in air at 500 °C for 24 h was different. As shown in figure 7 (a) and (b), the activity of the catalyst decreased in the first few hours and leveled off after about 10 h on stream. The selectivity for MA was quite constant, although there was a slight change in the CO/CO_2 ratio, being in favor of CO_2 with time-on-stream. The highest selectivity to maleic anhydride was 55%, which was obtained at 425 °C at a total gas flowrate of 70 ml/min.

Table 1 summarizes the reaction data obtained at relatively steady state for different activation procedures. At comparable conversions, the product selectivity at steady state was independent of the activation procedure.

3.2.3. Active phase in catalysts from precursor A

It has been widely accepted that butane oxidation on V–P–O catalysts takes place through a Mars and Van Krevelen redox mechanism involving lattice oxygen (scheme 1 below) [20,23]. During the reaction process, the surface active site undergoes reduction and oxidation in turn, by butane and oxygen.

Vanadium exists as V(IV) in the catalyst precursor ($VO(H_2PO_4)_2$). When the precursor was activated in air, the LRS spectra showed that an amorphous phase containing structural units like those formed in α-$VOPO_4$ appeared. Thus, at least some of the vanadium in the amorphous phase was oxidized to V(V). This was in agreement with the yellowish color of the air-calcined sample. When such sample was used for catalytic test in a gas mixture of butane/oxygen/He = 2/24/74 (vol%), its activity decreased with time-on-stream, together with the change in color indicating reduction of some V(V) to V(IV).

On the other hand, when the precursor was activated in the reactant mixture, a small amount of $VOPO_4$ phase was detected together with an amorphous phase. Thus, some vanadium was oxidized from V(IV) in the precursor to V(V) in the reaction mixture. We postulate that the increase in activity with time-on-stream (figure 6(a)) is associated with the slow build-up of V(V) in the catalyst. Since α-$VOPO_4$ is not a selective oxidation catalyst [24], the catalyst can only form a limited amount of this phase before degradation in selectivity becomes significant. The ability of this catalyst to retain the amorphous phase is important.

Thus, these data are consistent with the assumption that the catalytic activity for butane oxidation is closely correlated with the concentration of V(V) ions. The importance of V(V) in activating butane has been emphasized in the literature. In our early results, a correlation was also found between the catalytic activity of the vanadium pyrophosphate catalyst with its V(V) concentration [22]. Deterioration of maleic anhydride selectivity with increasing V(V) has also been documented [25].

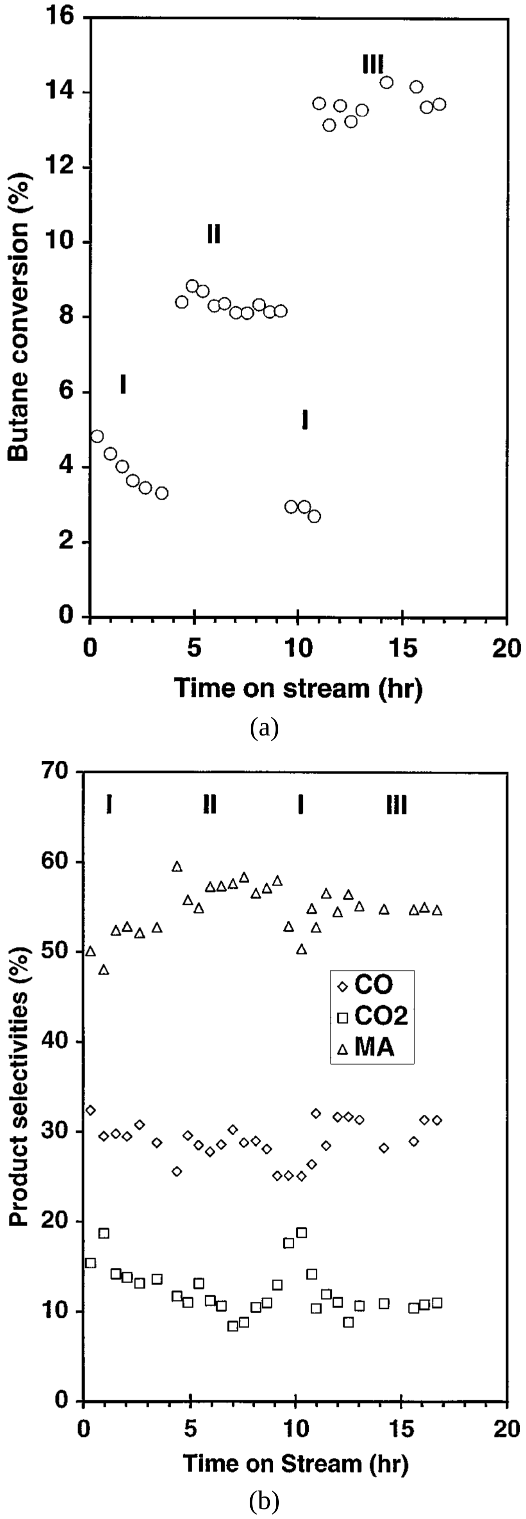

Figure 7. Butane oxidation on precursor A activated in air. Reaction conditions: catalyst weight = 1.7 g, butane/oxygen/He = 2/24/74 (vol%); period I: reaction temperature = 380 °C, gas flow rate = 70 ml/min; period II: 425 °C, 70 ml/min; period III: 425 °C, 40 ml/min. (a) Butane conversion and (b) product selectivities.

Table 1
Butane oxidation with precursor A derived bulk catalyst.[a]

Activation method	Reaction temperature (°C)	Mass of sample (g)	Butane conversion (%)	Selectivity[b] (%)					
				MA	AR	C_2	C_3	CO	CO_2
In situ	425	0.8	2	62	6	2	Trace	24	6
In situ	485	0.8	12	57	2	2	Trace	29	9
Air	425	1.7	8.4	57	2	2	Trace	28	11

[a] Total flow rate: 70 ml/min, $C_4H_{10}/O_2/He = 2/24/74$ (vol%).

[b] MA = maleic anhydride, AR = acrylic acid, C_2 = ethane; C_3 = propane.

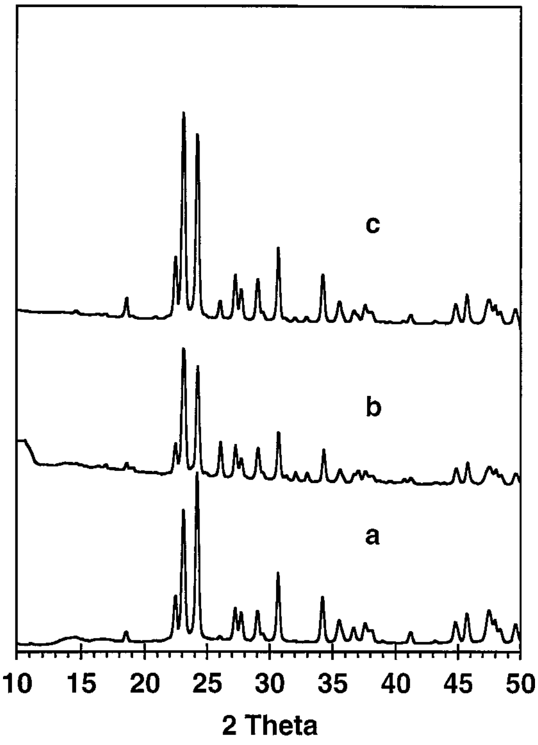

Figure 8. XRD patterns of catalysts derived from precursor B: (a) activated in the flow of 20 ml/min of butane/oxygen/He = 1.0/10.2/88.8 (vol%) at 400 °C for 4 h, (b) deactivated sample, and (c) re-oxidized after deactivation.

There was no detectable crystalline phase of vanadyl pyrophosphate in these samples, although maleic anhydride was produced with over 50% selectivity. Thus, crystalline vanadyl pyrophosphate is not a necessity for selective production of maleic anhydride.

3.3. Catalysts derived from precursor B

3.3.1. Catalyst structure

Activation of precursor B in the flow of 20 ml/min of butane/oxygen/He = 1.0/10.2/88.8 (vol%) at 400 °C for 4 h, produced a sample of a quite pure crystalline phase of $VO(PO_3)_2$. The XRD pattern of an activated catalyst is shown in figure 8, together with a deactivated and a regenerated sample. The XRD pattern of the activated sample agreed well with the one reported for $VO(PO_3)_2$ [13,18,19], except for a small bump at $2\theta = 26.2°$ that could be assigned to a tiny amount of $V(PO_3)_3$ [13,26].

The $VO(PO_3)_2$ phase was still the dominant phase in the deactivated catalyst (figure 8(b)). The more pronounced peaks at $2\theta = 26.2°$ and 33° suggested an increase in the amount of $V(PO_3)_3$. Heating the deactivated sample in flowing oxygen at 400 °C for 3 h partially regenerated the sample. The XRD pattern of this sample (figure 8(c)) showed a corresponding decrease in peak intensities at $2\theta = 26.2°$ and 33°, although they were still substantially more intense than those for the activated catalyst.

The LRS spectra shown in figure 9 (A) and (B) are consistent with the XRD results. A common set of dominant peaks was observed in all three samples at 960.9, 694.1, 1106.8, 1064.6, 394.7, 344.8, and 316 cm^{-1}, etc. (figure 9(A)) that could be assigned to crystalline $VO(PO_3)_2$ [13]. In the region 400–770 cm^{-1} (figure 9(B)), the intensities of a minor peak at about 671 cm^{-1} were different. According to the literature [13], $V(PO_3)_3$ has its strongest peak at 671.4 cm^{-1}. This peak was the strongest for the deactivated sample, and was undetectable in the activated catalyst.

3.3.2. Catalytic activity

The catalytic property of precursor B for butane oxidation was tested by activating the catalyst *in situ* under reaction conditions: in the flow of 20 ml/min of butane/oxygen/He = 1.0/10.2/88.8 (vol%) at 400 °C. The catalytic behavior of this sample is shown in figure 10. From the second hour on stream, the catalytic activity reached a steady state with about 4% butane conversion. After 3 h on stream, the butane conversion started to decrease and in about 6 h, it decreased to 0. Interestingly, as the catalyst deactivated, the selectivity changed accordingly. First, the selectivity to CO_2 decreased, and then the selectivities to CO and MA decreased. At the same time, the selectivity to furan increased. After the above reaction test, the catalyst color changed from greenish blue to green, which suggested the phase transformation from $VO(PO_3)_2$ to $V(PO_3)_3$ [27]. Treating the deactivated sample in flowing oxygen at 400 °C for 3 h only partially restored the catalytic property.

To test the oxygen insertion ability of the deactivated catalyst, 1-butene oxidation was carried out with the deactivated sample. The test was conducted at 400 °C using a feed of 50 ml/min 1-butene/oxygen/He = 1.5/24/74.5 (vol%). The results are shown in figure 11. The catalyst was only active for double-bond migration. No oxidation products could be detected. The 1-butene conversion

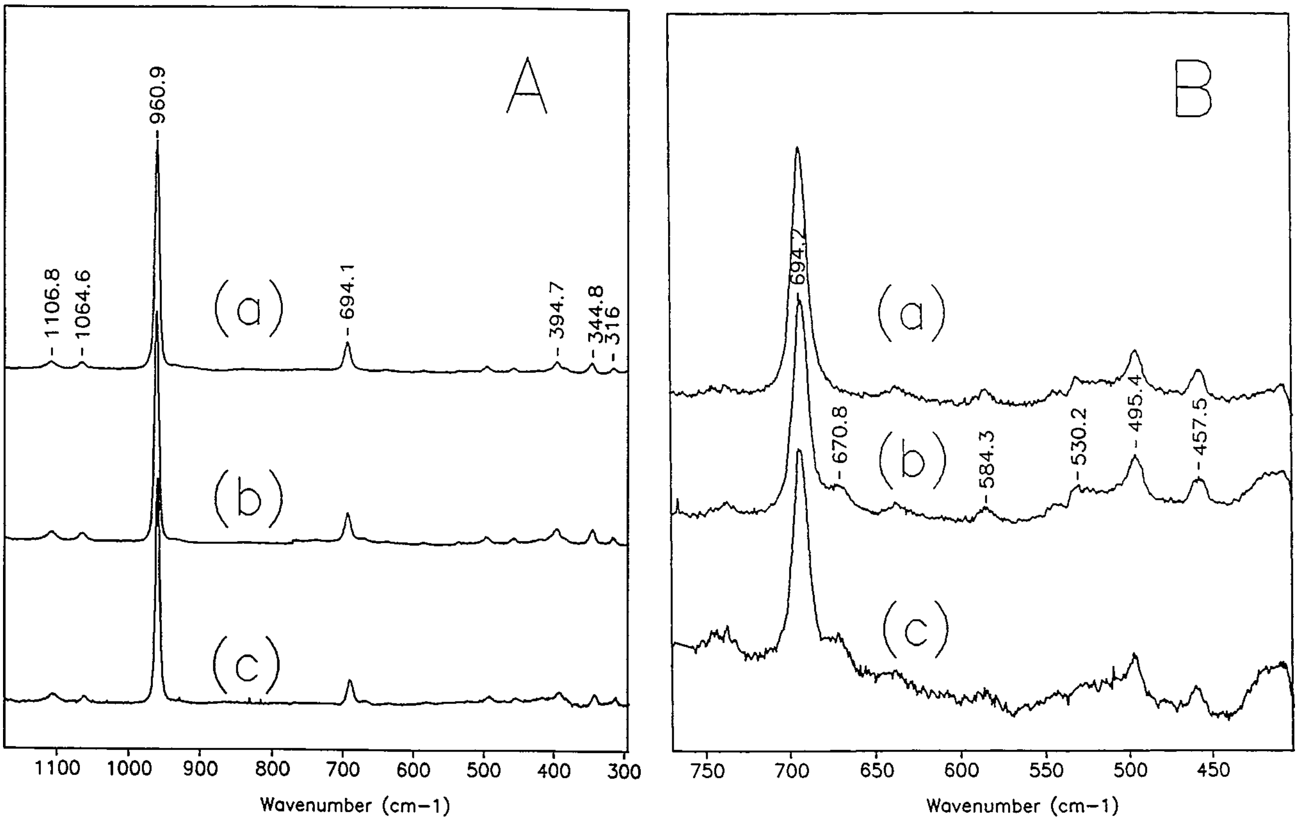

Figure 9. (A) LRS spectra of catalysts derived from precursor B: (a) activated sample (as in figure 10(a)), (b) deactivated sample, and (c) re-oxidized after deactivation. (B) LRS spectra of catalysts derived from precursor B: (a) activated sample (as in figure 10(a)), (b) deactivated sample, and (c) re-oxidized after deactivation.

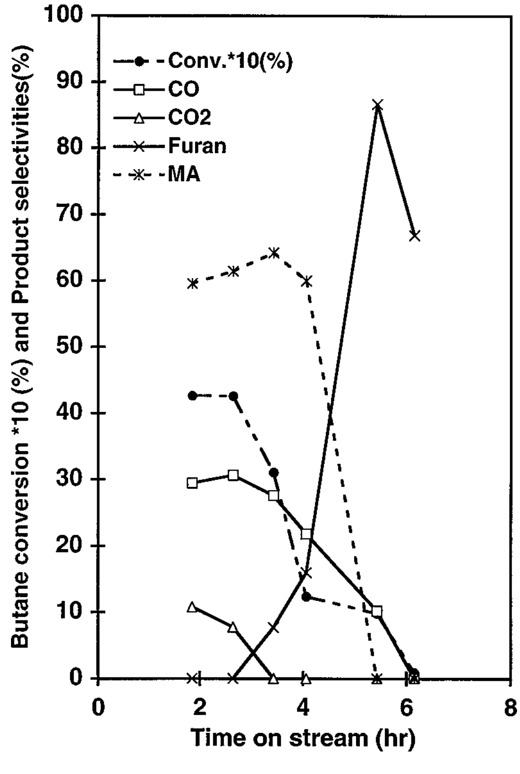

Figure 10. Butane oxidation on catalyst derived from precursor B. Reaction conditions: 20 ml/min of butane/oxygen/He = 1.0/10.2/88.8 (vol%) at 400 °C, 1.0 g of catalyst precursor.

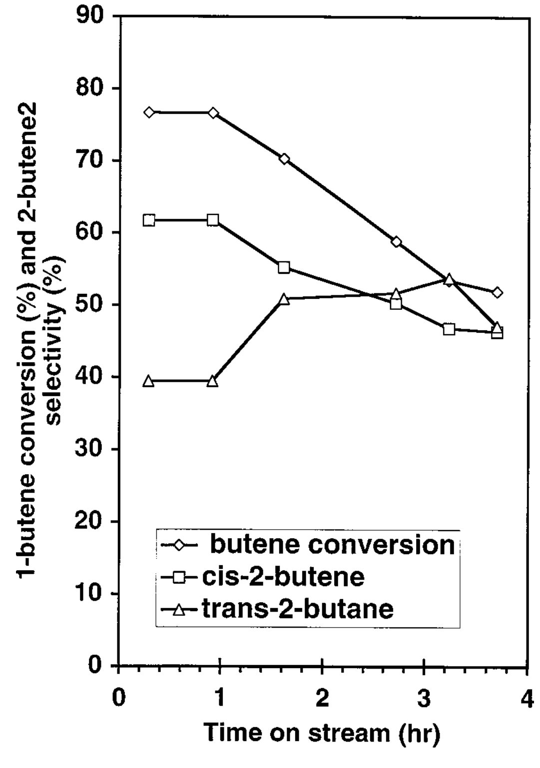

Figure 11. Butene oxidation on catalyst derived from precursor B after deactivation for butane oxidation (see figure 10). Reaction conditions: 400 °C with mixed gases of 1-butene/oxygen/He = 1.5/24/74.5 (vol%).

decreased from 76 to ∼50% in about 3 h. After the reaction test, the catalyst became black, indicating the formation of coke.

3.3.3. Active phase in catalysts from precursor B

These results can be explained using the redox scheme of vanadium:

$$\mathrm{V(V)} + \text{butane} \rightarrow \mathrm{V(IV)} + \text{surface intermediate} \quad (1)$$

$$\mathrm{V(IV)} + \text{surface intermediate} \rightarrow \mathrm{V(III)} + \text{products } (\mathrm{MA, CO, CO_2}) \quad (2)$$

$$\mathrm{V(III)} + (1/2)\mathrm{O_2} \rightarrow \mathrm{V(V)O} \quad (3)$$

$$2\mathrm{V(IV)} + (1/2)\mathrm{O_2} \rightarrow \mathrm{V_2(V)O} \quad (4)$$

$$\mathrm{V(III)} + 3\mathrm{PO_3} \rightarrow \mathrm{V(PO_3)_3} \quad (5)$$

Scheme 1. Redox scheme of vanadium during butane oxidation.

In this scheme, butane is activated by being oxidized on a V(V) surface site (step 1). A surface intermediate is formed, and the surface site is reduced to V(IV). Further reaction of the intermediate on a V(IV) site eventually forms the observed products in a multistep process, and V(III) may be formed in the process (step 2). At the same time, V(III) and V(IV) can be oxidized (steps 3 and 4). However, if free phosphate groups are present, such as in samples with P/V larger than two, $V(PO_3)_3$ can be formed also.

Precursor B was transformed readily into crystalline $VO(PO_3)_2$ under reaction conditions. The large excess of phosphorus might have facilitated this transformation compared with precursor A. Consequently, there was only a small concentration of V(V) in the activated sample and the sample was much less active than catalysts from precursor A.

Continued exposure to the reaction mixture caused reduction of the sample. The small amount of V(V) was reduced to V(IV) and V(III), and $V(PO_3)_3$ was formed. As a result, the catalyst deactivated. That this occurs suggests that the reoxidation rate of the sample was slow, which agrees with the fact that oxidation at 400 °C for 3 h could not fully reoxidize or regenerate the catalyst. The deactivated sample did not have oxidation activity, although it was active for double-bond isomerization.

The LRS and XRD results showed that the dominant crystalline phase of the deactivated sample was $VO(PO_3)_2$. Assuming that this phase was not formed rapidly when the sample was exposed to air, and that the sensitivity factors for $VO(PO_3)_2$ and $V(PO_3)_3$ are comparable for both techniques, the amount of crystalline $V(PO_3)_3$ in the deactivated catalyst was estimated to be less than 10%. Therefore, the formation of crystalline $V(PO_3)_3$ must be in the near surface region. And the transfer of lattice oxygen to the surface from the $VO(PO_3)_2$ underneath the surface layer was slow.

The low activity and slow deactivation permitted observing the change in product distribution at very low butane conversions (figure 10). The data were consistent with the scheme that furan is an intermediate oxidation product, which is further oxidized to maleic anhydride [9,24,28]. In addition, there is a parallel combustion pathway.

A comparison of the results obtained on catalysts from precursors A and B shows that, at a P/V ratio near 2, the catalyst structure and its catalytic performance are very sensitive to the P/V ratio. Excess phosphate facilitates the transformation of $VO(H_2PO_4)_2$ to a crystal phase of $VO(PO_3)_2$ and the formation of $V(PO_3)_3$ under reaction conditions. The controversial results in the literature on the catalytic performance of such catalysts may originate from the slightly different P/V ratios in those catalysts. It should be noted that the active catalysts reported in literature derived from $VO(H_2PO_4)_2$ always contain some amounts of amorphous phases in addition to $VO(PO_3)_2$ [8–10].

4. Conclusions

The transformation of a V–P–O precursor of $P/V \geqslant 2$ depends strongly on the presence of excess P. For $P/V \approx 2$, a poorly crystalline sample was formed, which could be oxidized relatively easily. If excess P is present, crystalline $VO(PO_3)_2$ is formed much more easily, and the oxidation of V(IV) to V(V) becomes much slower. As a result, the catalyst is less active in butane oxidation, and it deactivates with time-on-stream with the formation of $V(PO_3)_3$. This dependence of the properties on the presence of excess phosphorus may explain the different behaviors of $VO(PO_3)_2$ reported in the literature. The results also show that vanadyl pyrophosphate in not a necessary component of a selective butane oxidation catalyst.

Acknowledgement

Financial support of this work by the US Department of Energy, Basic Energy Science is gratefully acknowledged.

References

[1] G. Centi, Catal. Today 16 (1993) 5.

[2] E. Bordes, Catal. Today 16 (1993) 27.

[3] G.J. Hutchings and R. Higgins, J. Catal. 161 (1996) 153.

[4] M. Ruitenbeek, A.J. van Dillen, D.C. Koningsberger and J.W. Geus, in: *Preparation of Catalysts VII*, Stud. Surf. Catal., Vol. 118 (Elsevier, Amsterdam, 1998) p. 295.

[5] G.J. Hutchings, C.J. Kiely, M.T. Sananes-Schulz, A. Burrows and J.C. Volta, Catal. Today 40 (1998) 273.

[6] N. Harrouch Batis, H. Batis, A. Ghorfel and J.C. Volta, J. Catal. 128 (1991) 248.

[7] F. Garfacci, J.C.J. Bart, R. Tassinari, G. Vlaic and P. Lagarade, J. Catal. 98 (1986) 317.

[8] K.E. Birkeland, S.M. Babitz, G.K. Bethke, H.H. Kung, G.W. Coulston and S.R. Bare, J. Phys. Chem. B 101 (1997) 6895.

[9] J.M.C. Bueno, G.K. Bethke, M.C. Kung and H.H. Kung, in: *15th Simposio Iberoamericano de Catalisis*, Cordoba, Argentina, September 1996, paper B-4.

[10] H. Morishige, J. Tamaki, N. Miura and N. Yamazoe, Chem. Lett. (1990) 1513.

[11] M.T. Sananes, G.J. Hutchings and J. Volta, J. Catal. 154 (1995) 253.

[12] G.J. Hutchings, M.T. Sananes, S. Sajip, C.J. Kiely, A. Burrows, I.J. Ellison and J.C. Volta, Catal. Today 33 (1997) 161.

[13] V.V. Guliants, J.B. Benziger, S. Sundaresan, I.E. Wachs, J.-M. Jehng and J.E. Roberts, Catal. Today 28 (1996) 275.

[14] G.K. Bethke, D. Wang, J.M.C. Bueno, M.C. Kung and H.H. Kung, Stud. Surf. Sci. Catal. 110 (1997) 453.

[15] F.K. Hannour, A. Martin, B. Kubias, B. Lucke, E. Bordes and P. Courtine, Catal. Today 40 (1998) 263.

[16] G. Villeneuve, A. Erragh, D. Beltran, M. Drillon and P. Hagenmuller, Mater. Res. Bull. 12 (1986) 621.

[17] G.Z. Ladwig, Chemistry 8 (1968) 307.

[18] E. Bordes, Catal. Today 1 (1987) 499.

[19] A.V. Lavrov, Inorg. Mater. (May 1975) 1869.

[20] D. Wang, H.H. Kung and M.A. Barteau, in: *The 16th North American Meeting of Catalysis Society*, 30 May–4 June 1999, Boston.

[21] K.E. Birkeland, Ph.D. thesis, Northwestern University (1995).

[22] G.W. Coulston, S.R. Bare, H. Kung, K. Birkeland, G.K. Bethke, R. Harlow, N. Herron and P.L. Lee, Science 275 (1997) 191.

[23] M. Abon, K.E. Bere and P. Delichere, Catal. Today 33 (1997) 15.

[24] T. Shimoda, T. Okuhara and M. Misono, Bull. Chem. Soc. Jpn. 58 (1985) 2163.

[25] G.J. Hutchings, A. Burrows, S. Sajip, C.J. Kiely, K.E. Beres, J.C. Volta, A. Tuel and M. Abon, in: *Proc. 3rd World Congr. Oxidn. Catal.*, Stud. Surf. Sci. Catal., Vol. 110 (Elsevier, Amsterdam, 1997) p. 209.

[26] B.C. Tofieldand and G.R. Crane, J. Chem. Soc. Dalton Trans. (1975) 1806.

[27] F. Cavani and F. Trifirò, CHEMTECH (1994) 18.

[28] M. Pepera, J.L. Callahan, M.J. Desmond, E.C. Milberger, P.R. Blum and N.J. Bremer, J. Am. Chem. Soc. 107 (1985) 4883.